Effect of Attitude Constraints on Solar-Electric Geocentric Transfers

Lester L. Sackett* and Theodore N. Edelbaum†
The Charles Stark Draper Laboratory, Inc., Cambridge, Mass.

Attitude constraints on both the thrust vector and the plane of the solar cell arrays have been considered for vehicles such as the SERT-C solar electric propulsion spacecraft. The attitude constraints introduce complications because power becomes a function of position and attitude and because the maneuverability domain may be nonconvex. Corners with control switchings may exist. A derivation of a nearly optimal control is presented for the attitude-constrained case of zero pitch and roll. This suboptimal control is nearly time optimal but uses less fuel than the time-optimal solution. Comparisons are made between the constrained and unconstrained cases. Dependence of flight time and ΔV on launch time of day is shown for a particular spacecraft example. Other characteristics of a particular trajectory are illustrated.

Introduction

MOST of the geocentric trajectory analyses for solar electric spacecraft have assumed fully articulated spacecraft where the solar array and the thrust vector both can be pointed in their respective optimum directions.[1-4] However, it may be desirable to introduce constraints on the solar panel or thrust orientation in order to simplify vehicle design or to reduce attitude sensor requirements. An example of such constraints is one of the SERT-C designs.[5] This particular design constrains the thrust vector to yaw motion in a plane at right angles to the radius vector. The solar panels can rotate around an axis that is orthogonal to both the radius vector and the thrust vector. Such a design reduces attitude sensor requirements.[5] However, it couples the power developed to the thrust direction. Most thrust orientations do not allow maximum power to be developed. The flight time is increased both because of this coupling and because of the thrust direction constraint.

The present paper is intended to assess the increase in flight time and fuel consumption due to introducing these attitude constraints. Nearly time-optimal trajectories are generated for both the constrained and unconstrained cases. The unconstrained cases were generated with the code described in Refs. 1 and 6-8. The constrained cases were generated with the code described in Refs. 9 and 10. The discussion in this paper is limited to thrusting in an inverse square gravity field.

To obtain trajectories for the attitude-constrained problem, the method of averaging is used in combination with a nonsingular set of orbital elements, the equinoctial orbital elements.[11] Optimization is carried out by the indirect method, with the resulting two-point boundary-value problem being solved by a shooting method.

Problem Statement

Consider a spacecraft in Earth orbit where the roll axis lies in the orbit plane and is perpendicular to the Earth-spacecraft radius vector; the yaw axis is parallel to the Earth radius vector and directed toward the Earth; the pitch axis is perpendicular to the orbit plane and directed south. For the nominal attitude, the principle body-centered axes are aligned with this coordinate system. The ion thrusters are mounted on the negative roll face of the spacecraft and directed parallel to the roll axis. The solar arrays are flat panels and are capable of rotation about their longitudinal axis, which is aligned with the spacecraft pitch axis. The required low thrust directions are achieved entirely by the spacecraft attitude rotations.

The thrust vector must have no component along the vector from Earth to spacecraft. The thrust direction is determined by one control variable, the yaw angle. Since pitch and roll are constrained to be zero, the orientation of the axis of the solar panels is determined by the yaw angle. The panels are allowed to rotate about this axis, resulting in one more control variable, called θ. Power is assumed to be proportional to the cosine of the angle (ϕ) between the normal to the panels and the line to the sun so that

$$P=P_0\cos\phi$$

For the purposes of this paper, P_0 will be assumed to be a constant, although, in fact, there are other effects such as power degradation due to Van Allen radiation.[12] The angle ϕ is a function of the two control angles, the yaw angle and the panel rotation angle. The geometric relation is developed later.

The initial state is given, and it is desired to reach a final subset of the state at some unspecified, final time. A particular suboptimal control, which is nearly time optimal, is derived. A costate formulation is used, along with the method of averaging, to set up a two-point boundary-value problem that can be solved by using a Newton method to iterate on the unknown initial costate and value of the final time in order to meet the desired final conditions on the state and costate.

State and Costate Formulation

The unaveraged variation of parameters equation for the five slowly varying orbital elements is given by

$$\dot{z}=(2P/mc)M(z,F)\hat{u} \tag{1}$$

where five equinoctial orbital elements compose the vector z. A sixth orbital element, the eccentric longitude ($F=\omega+\Omega+E$, where ω, Ω, and E are the argument of perigee, the longitude of the ascending node, and the eccentric anomaly, respectively), will be eliminated by averaging. P is the power, c is the constant exhaust velocity, m is spacecraft mass, M is the partial of the orbital elements with respect to velocity (written out in detail in Ref. 1), and $\hat{u}$ is the unit thrust direction vector. (The caret over a vector denotes a unit vector). The mass flow rate equation is given by

$$\dot{m}=-2P/c^2 \tag{2}$$

Presented as Paper 75-350 at the AIAA 11th Electric Propulsion Conference, New Orleans, La., March 19-21, 1975; submitted April 7, 1975; revision received Nov. 3, 1975. The authors wish to acknowledge the contribution of James Cake, Lewis Research Center, Cleveland, Ohio, as the NASA Technical Monitor on Contract NAS 3-18886, which supported this work.

Index categories: Earth-Orbital Trajectories; Navigation, Control, and Guidance Theory; Electric and Advanced Space Propulsion.

*Staff Member. Member AIAA.

†Staff Member. Associate Fellow AIAA.

The full six-dimensional state x includes z and m.

Next the unaveraged Hamiltonian is written. Then the averaged Hamiltonian is formed, from which the derivatives of the approximate state and costate can be obtained. Those equations are used to generate a trajectory once a control has been determined. The unaveraged Hamiltonian is given by

$$H(x,\lambda,F,t,\theta,\psi) = \lambda_z{}^T \dot{z} + \lambda_m \dot{m} \tag{3}$$

Note here that P is a function of the yaw angle, called ψ, and the panel orientation angle θ. The thrust direction $\hat{u}$ is determined by the yaw angle ψ. These control angles are not yet determined.

The averaged Hamiltonian is given by

$$\bar{H}(\bar{x},\bar{\lambda},t) = \frac{1}{T_0}\int_0^{T_0} H(\bar{x},\bar{\lambda},F(t),\bar{t},\theta,\psi)\,dt \tag{4}$$

$$= \frac{1}{2\pi}\int_0^{2\pi} H(\bar{x},\bar{\lambda},F,\bar{t},\theta,\psi)\,\frac{dt}{dF}\,(\bar{x},F)\,dF$$

where T_0 is the orbital period, and the overbar indicates approximate quantities. The $\bar{t}$ dependence refers to time dependence which is independent of spacecraft motion such as Earth motion around the sun. In practice, integration with respect to F is more convenient. Then the derivative equations for the state and costate are given by

$$\dot{x} = \frac{\partial \bar{H}^T}{\partial \bar{\lambda}} = \frac{1}{2\pi}\int_0^{2\pi} \frac{\partial H^T}{\partial \bar{\lambda}}\,\frac{dt}{dF}\,dF \tag{5}$$

$$\dot{\lambda}^T = -\frac{\partial \bar{H}}{\partial \bar{x}} = \frac{-1}{2\pi}\int_0^{2\pi}\left[\frac{\partial H}{\partial \bar{x}}\,\frac{dt}{dF} + H\frac{\partial}{\partial \bar{x}}\left[\frac{dt}{dF}\right]\right]dF \tag{6}$$

These equations hold for a suboptimal control. The partials inside the integral can be obtained by using the chain rule on Eq. (3). The partial of M with respect to z as well as the partial of dt/dF are given in Ref. 9. Other partials depend on the precise statement of the dependence on θ and ψ. That dependence is developed in the next section.

Geometry

It is convenient to define a special coordinate system by the following basis vectors:

$$\hat{e}_3 = -\hat{r} \tag{7}$$

where r is the Earth-to-spacecraft vector, and $\hat{e}_1$ is in the plane defined by the radius vector and the Earth-sun vector R_s (assumed equivalent to the spacecraft-sun vector). In particular

$$\hat{e}_2 = \hat{e}_3 \times \hat{R}_s / |\hat{e}_3 \times \hat{R}_s| \tag{8}$$

$$\hat{e}_1 = \hat{e}_2 \times \hat{e}_3 \tag{9}$$

In this system, the sun direction is defined by the angle β, where

$$\hat{R}_s = \cos\beta \hat{e}_3 + \sin\beta \hat{e}_1 \tag{10}$$

(In the equinoctial system, $\cos\beta = -\hat{r}^T \hat{R}_s$.) The thrust acceleration vector direction is constrained to the $\hat{e}_1 - \hat{e}_2$ plane and given in terms of the angle ψ with respect to the $\hat{e}_1$ axis by the unit vector

$$\hat{u} = \cos\psi \hat{e}_1 + \sin\psi \hat{e}_2 \tag{11}$$

This vector also can be written as

$$u = T\begin{bmatrix}\cos\psi\\ \sin\psi\\ 0\end{bmatrix} \tag{12}$$

where

$$T = [\hat{e}_1 \hat{e}_2 \hat{e}_3] \tag{13}$$

The power yield of the solar panels is proportional to the cosine of the angle betwen the normal to the panels and the vector pointing toward the sun. The panels can rotate about an axis that is in the $\hat{e}_1 - \hat{e}_2$ plane and is assumed to be perpendicular to $\hat{u}$. The normal to the panels can be defined in terms of ψ and an angle of rotation θ about this axis in the $\hat{e}_1 - \hat{e}_2 - \hat{e}_3$ system, namely

$$\hat{N} = \sin\theta\cos\psi \hat{e}_1 + \sin\theta\sin\psi \hat{e}_2 + \cos\theta \hat{e}_3 \tag{14}$$

The cosine of the angle between the normal and the sun vector is given by

$$\cos\phi = \hat{N}^T \hat{R}_s = \sin\beta\sin\theta\cos\psi + \cos\theta\cos\beta \tag{15}$$

Thus we have established completely the dependence of power and thrust direction on the control angles θ and ψ.

The costate equations require the partials of $\cos\phi$ and thus of β and $\hat{r}$. As formulated here, the partial of T is needed, although, if a constraint equation is used, only the partial of $\hat{e}_1$ is needed. Details of these straightforward partials are given in Ref. 9.

Derivation of the Control Angles

Taking into account the relations established in the previous section, the Hamiltonian of Eq. (3) can be written out in more detail as

$$H = \frac{2P_0}{c}\cos\phi\left[\lambda_z^T \frac{MT}{m}\begin{bmatrix}\cos\psi\\ \sin\psi\\ 0\end{bmatrix} - \frac{\lambda_m}{c}\right] \tag{16}$$

where the dependence of $\cos\phi$ on θ and ψ was given in Eq. (15). The optimal θ is found by maximizing H with respect to θ. This is equivalent to maximizing $\cos\phi$. This maximizing is straightforward and results in $\cos\phi$ as a function of β and ψ

$$\cos\phi = (1 - \sin^2\beta\sin^2\psi)^{1/2} \tag{17}$$

It is interesting to look in the $\hat{e}_1 - \hat{e}_2$ plane at the locus of the vector pointing along the thrust direction with magnitude equal to $\cos\phi$. For each β, there is a curve in the $\hat{e}_1 - \hat{e}_2$ plane as ψ varies from 0° to 360°. These curves are symmetric about both axes and repeat for every β interval of 90°. Note that, for $|\cos\beta| < (2)^{-1/2}$, the constant β curves are concave, and for $|\cos\beta| > (2)^{-1/2}$ they are convex (see Fig. 1). Since power is a function of thrust direction, this curve will be important in determining the desired control angle ψ that specifies the thrust direction.

The Hamiltonian is now only a function of one control ψ, which determines the thrust direction. In Eq. (16), the quan-

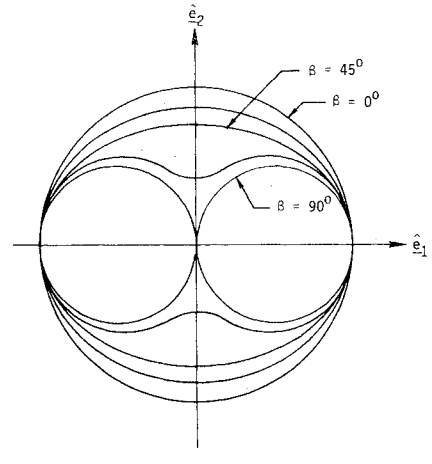

Fig. 1 P/P_0 locus.

tity $T^T M^T \lambda_z$ is just the primer vector given in the $\hat{e}_1 - \hat{e}_2 - \hat{e}_3$ system and will be designated as λ_v with components λ_{v1}, λ_{v2}, λ_{v3}. Equation (16) can be rewritten as

$$H = \frac{2P_0}{c} (1 - \sin^2\beta \sin^2\psi)^{1/2} \left[\frac{\lambda_{v1}}{m} \cos\psi + \frac{\lambda_{v2}}{m} \sin\psi - \frac{\lambda_m}{c} \right] \quad (18)$$

For a minimum time solution, this Hamiltonian must be maximized with respect to ψ. If this is done by setting $\partial H/\partial\psi = 0$ and converting all $\sin\psi$ to $\cos\psi$, a sixth-order polynomial in $\cos\psi$ results.

If power were not a function of ψ (i.e., $\cos\phi = 1$), then the optimal thrust direction would be along the projection of the primer vector onto the $\hat{e}_1 - \hat{e}_2$ plane. Minimum time and minimum fuel trajectories would be identical. When power dependency on ψ is included, a lower power may result if thrust is along the primer projection. Consequently, the time-optimal procedure is to bias the thrust vector away from the primer direction in the direction of higher power. The bias is selected such that the increased power more than offsets the loss due to inefficient thrust pointing; i.e., the projection of the optimal vector onto the primer direction is greater than the thrust vector that would occur if thrusting were along the primer direction. The value of λ_m affects the bias so as to increase power (compared to zero λ_m) and therefore mass flow rate further. The lower spacecraft mass then can be accelerated to the final state more quickly than if the effect of λ_m were not included.

Is the minimum time solution really desirable for this problem? We think not. Consider what happens if the part of the Hamiltonian containing λ_m is ignored, and instead we maximize

$$H' = (2P_0/c) (1 - \sin^2\beta \sin^2\psi)^{1/2} (\lambda_{v1} \cos\psi + \lambda_{v2} \sin\psi) \quad (19)$$

In the $\hat{e}_1 - \hat{e}_2$ plane, one can see that this is equivalent to maximizing the projection of the vector $(\cos\psi)(1 - \sin^2\beta \sin^2\psi)^{1/2}$ onto the $\hat{e}_1 - \hat{e}_2$ components of the primer vector $(\lambda_{v1}, \lambda_{v2})$. The locus of the first vector is just that shown in Fig. 1. The maximization then can be carried out using analytical geometry. It also is possible to obtain the control by setting $\partial H'/\partial\psi = 0$. If $\sin\psi$ is converted to $\cos\psi$, this results in a sixth-order polynomial in $\cos\psi$, but with the coefficients of all odd powers equal to zero. This equation can be converted to a cubic in $\tan\psi$ (where we define $\tan\alpha = \lambda_{v2}/\lambda_{v1}$):

$$\cos^2\beta \tan^3\psi + (2\sin^2\beta - 1)\tan\alpha \tan^2\psi + (1 + \sin^2\beta) \tan\psi\psi - \tan\alpha = 0 \quad (20)$$

Dividing by $\cos^2\beta$, this also can be written as

$$\tan^3\psi + (\tan^2\beta - 1)\tan\alpha \tan^2\psi + (2\tan^2\beta + 1) \tan\psi - (1 + \tan^2\beta)\tan\alpha = 0 \quad (21)$$

This suboptimal thrust direction results in a lower power and a corresponding lower mass flow rate, but for a longer time. Analysis of the worst-case example (see Appendix) indicates that the time penalty is small while actually resulting in a fuel savings compared to the time-optimal control, since the lower mass flow rate more than makes up for the additional fuel consumption dictated by the longer flight time. In addition, the control is much easier to calculate, since the solution to the cubic equation can be obtained analytically, unlike the solution to the sixth-order polynomial. This saves computer time. Thus it was decided to use this control law for the present study.

This control law has some interesting characteristics. Figure 2 shows curves of constant α superimposed on the curves of Fig. 1 for one quadrant. Thus, for a given β (sun angle) and α (primer vector angle), the resulting ψ is just the angle made by the line from the origin to the intersection of the appropriate α and β curves. Note that in this quadrant ψ is always less than α except for $\beta = 0$ when $\psi = \alpha$ or for $\beta < 45°$ and $\alpha = 90°$ when also $\psi = 90°$; when $\beta = 90°$, $\psi \to 45°$ as $\alpha \to 90°$. For $\beta > 45°$, as α crosses the $\hat{e}_2$ axis there is a jump in ψ to a symmetrical position in the adjoining quadrant. If α remains aligned with the $\hat{e}_2$ axis for a finite time, a singular arc results. Since it would be nonoptimizing (in terms of H') to operate on the concave portions of the curves, a chattering solution is required as ψ jumps back and forth in the two quadrants in infinitesimal time, yielding a resultant thrust vector along the $\hat{e}_2$ axis. In practice, this solution probably never will be required (as well as being impossible to implement if it were). Jumps in the control direction can and do occur, however, The locus of points on Fig. 2 at which a jump occurs is given by an arc of a circle of radius $(2)^{-1/2}$ and center at the origin. The ψ at which a jump occurs is related to β by the relation

$$\cos^2\psi = (\sin^2\beta - 1/2)/\sin^2\beta \quad (22)$$

In practice, then, β and α are calculated, and the coefficients of Eq. (21) are obtained. The cubic equation then can be solved analytically. Appropriate modifications must be made if the tangents are very large or infinite. There are three roots to the cubic equation, and if all three are real they correspond to six possible values of ψ in a 360° range. These correspond to various maxima and minima. The one angle of interest is in the same quadrant as α, and none of the other solutions are. Thus we can obtain the control angle ψ, which then can be substituted into the equations of motion. This calculation must be made at each quadrature point on an orbit.

Because of the numerical inaccuracy of using a quadrature over a region that contains a discontinuity in the integrand, it is best to calculate possible jump points and then do separate quadratures between these points. A jump in the thrust direction occurs when the projection of the primer vector onto the $\hat{e}_1 - \hat{e}_2$ plane passes from one side of $\hat{e}_2$ to the other. At the time of crossing, the projection is perpendicular to $\hat{e}_1$ and also perpendicular to $\hat{R}_s$. Thus, the condition for a jump can be written as

$$[\lambda_{v1}, \lambda_{v2}, 0]\hat{R}_s = 0 \quad (23)$$

An actual jump occurs only if the constant β curve is concave, i.e., $|\cos\beta| < (2)^{-1/2}$. Equation (23) can be reduced to a sixth-order polynomial in $\cos F$ (where F is the eccentric longitude of the spacecraft in its orbit). If all roots are real, there can be 12 values of F, six of which are extraneous, arising from a squaring when deriving the polynomial. If the orbit is circular, there can at most be four values of F for which jumps may occur (unless there is a singular arc). In practice, there

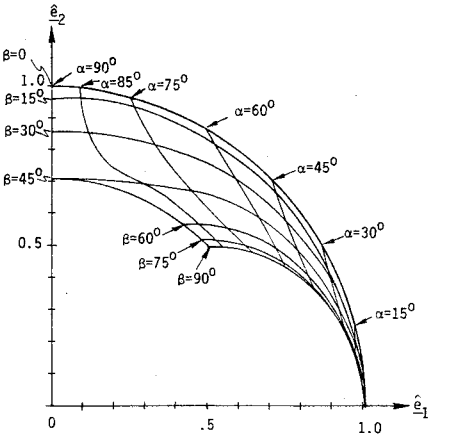

Fig. 2 Lines of constant primer angle (α) and sun angle (θ).

usually seem to be only two. For the results given in this paper, the method used to find the values of F for which a jump might occur was to divide the 360° range of F into small equal intervals and then to check to see if there was a sign change of Eq. (23) from one side of an interval to the other side. If so, the exact F within the interval for which Eq. (23) was zero was found by using a nonlinear function root-finding routine.

Trajectory Generation

The derivative equations for the approximate state and costate of Eqs. (5) and (6) are integrated to generate a trajectory. The integration of the approximate state and costate equations is performed with a Runge-Kutta integrator. At each integration point, the averaging integral is performed by a gaussian quadrature. Prior to the quadrature, possible jump points are calculated, and a separate quadrature is performed between the values of F where jumps may occur. (For the results in this paper, there were two intervals). At each evaluation point of the integrand of the quadrature, the thrust direction was calculated by solving the cubic of Eq. (21).

The single trajectory generation portion of the code is coupled with a Newton iterator to solve the two-point boundary-value problem. The initial costate and value of the final time are iterated on in order to meet the final conditions, which are functions of the final state and costate (usually a specified semimajor axis, eccentricity, and inclination and the appropriate transversality conditions). The partial derivative matrix of final conditions with respect to the initial costate is obtained numerically by calculating neighboring trajectories to a nominal.

Results

Several SERT-C-type cases were run. All of these assume only the inverse square gravitational field with or without attitude constraints. Comparisons are made between the unconstrained case and attitude-constrained cases while varying launch time. A particular constrained example is looked at in greater detail. These cases assume an initial orbit with $a=$ 9528.16 km, $e=0$, $i=28.3°$, an initial mass of 849.6 kg, maximum power = 4.828 kW, and specific impulse = 2900 sec. The final orbit is equatorial geosynchronous. These cases were run with a 10-day time step and averaged around an orbit using either two 4-point or two 8-point quadratures. The variation in resulting flight times and ΔV's from using sets of 4- or 8-point quadratures was less than 0.5%.

The effect of varying the time of launch during a day for the constrained case can be shown by varying the initial longitude of the ascending node. This effect is illustrated in Fig. 3 for a launch date of March 21.5, 1980. The flight time (t_f) and ΔV are plotted vs initial longitude of ascending node. The dotted line indicates the unconstrained value. The flight time varies by about 18 days, with a minimum of 130 days around $\Omega = 135°$ compared to the unconstrained value of 124 days. The range of increased flight time over the unconstrained case is from about 5 to 20%. The unconstrained ΔV is 4.65 km/sec, and the constrained cases vary from less than 1% to about 12% greater. In the minimum case, about 15% of the initial mass was consumed. This was only about 0.6 kg more than the unconstrained case. Similar results follow when varying day of launch over a year for a fixed time of day. The $\Omega = 135°$ case, which results in the lowest flight time and ΔV, will be looked at in greater detail. The semimajor axis and inclination histories for this case and the unconstrained case are plotted in Fig. 4.

Figure 5 shows yaw plotted as a function of eccentric longitude for the initial and the final orbits. Because of the coupling with power, the maximum does not occur at exactly the line of nodes (which would be 135° and 315°) as in the unconstrained case. There are two jumps in yaw of about 60° for the final orbit. This will be discussed further. For this circle-to-circle transfer, the pitch angle for the unconstrained case is always zero, and so the effect of the pitch constraint is not illustrated.

Figure 6 shows a plot of the ratio of power to maximum power vs eccentric longitude for the initial and final orbits. For the initial orbit, the power is near maximum for nearly the entire orbit, dropping to a minimum of 0.91 but with an

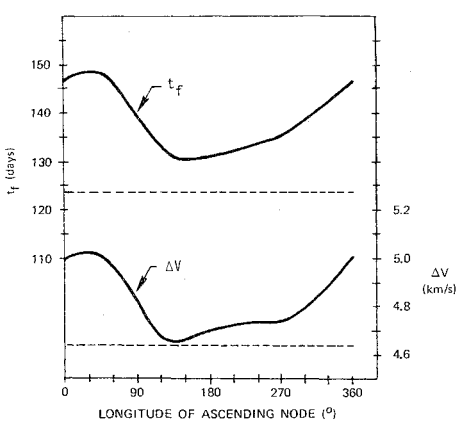

Fig. 3 Flight time and ΔV vs nodal angle.

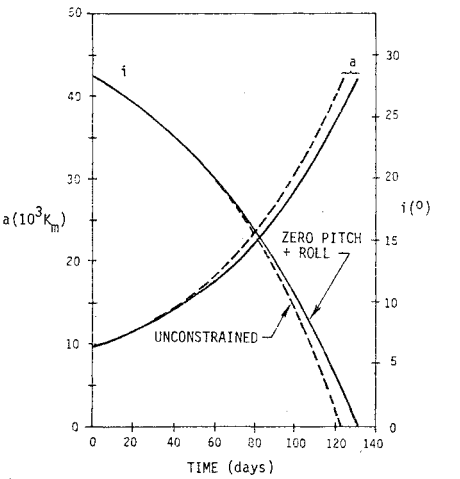

Fig. 4 Semimajor axis and inclination histories.

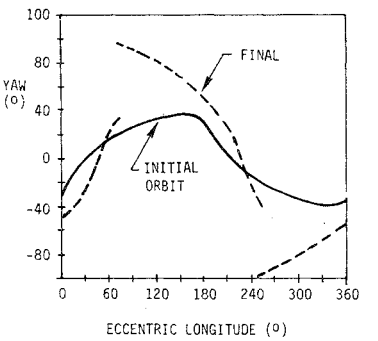

Fig. 5 Yaw for initial and final orbits.

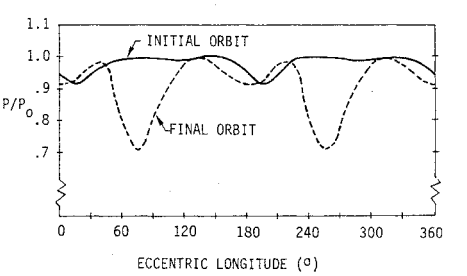

Fig. 6 Ratio of power to maximum power for initial and final orbits.

average of 0.98. For the final orbit, the minimum reaches 0.707, which is the absolute minimum possible and which occurs at a jump point of the control. Even so, the average power ratio is over 0.9. The two other relative minimums for each orbit occur near the minimum and maximum of the primer vector angle (α) (and also the thrust angle ψ).

In Fig. 7 are plotted the primer vector angle (α), the thrust angle (ψ), and the sun angle (β) for the initial orbit. These angles are defined in the $\hat{e}_1 - \hat{e}_2 - e_3$ system. The sun angle is the angle between the radius vector and the line to the sun and can vary by at most 180°, depending on the orientation of the orbit. For the initial orbit, the variation is approximately 140°. The thrust angle is a function of α and β and is equal to α at $\alpha=0°$ and 180°. For this orbit, $\psi=90°$ when $\alpha=90°$. Since $\beta \approx 157°$ and 23° for the two positions at which $\alpha=90°$, there is no jump in ψ (for a jump $45° < \beta < 135°$).

The primer vector angle (α), thrust angle (ψ), and sun angle (β) are plotted for the final orbit in Fig. 8. Obviously for this orbit there is a jump in ψ when $\alpha=90°$. Note that at this point $\beta \approx 124°$ for the first jump, and $\beta \approx 56°$ for the second. For these values of β, the jump in ψ is approximately 60°. It is interesting to note that after the first jump ψ decreases slightly even as α increases (ψ increasing as α decreases after the second jump), as the changing β allows a closer alignment with the primer vector at less power loss penalty. Jumps in ψ occur during about the last 20 days of the trajectory.

Conclusions

In this paper, we have described a suboptimal control for use with attitude-constrained solar electric geocentric transfers which is nearly time optimal without wasting fuel. Without the roll constraint, but with a pitch constraint, power would not be a function of thrust direction, and so the time-optimal thruster direction would be along the projection of the primer vector in the plane normal to the radius vector. The roll constraint causes power to become a function of thrust angle and sun angle. For certain sun angles, the locus of the ratio of power to maximum power is concave, and thus there may be jumps in the the control angle. The minimum power ratio is $(2)^{-1/2}$, but examples indicate that the average ratio is usually 0.9 or higher.

Comparisions were made for a SERT-C-type mission between constrained and unconstrained cases for an inverse square gravity field. Flight time and ΔV vary for the constrained cases as a function of launch date and time of day. A launch time can be found for which the constrained ΔV is less than 1% and the time of flight less than 5% more than the unconstrained case. An important difference between the constrained and unconstrained cases was the discontinuities in thrust direction and panel orientation angle for the constrained case which occurred during the last 20 days of a 130-day mission. Operationally, such instantaneous changes could not be performed. The finite time required for an attitude change would degrade the results given here somewhat.

Appendix: Worst-Case Evaluation of Suboptimal Approximation

In the section on "Control Angles," two reasons were given for utilizing a suboptimal approximation where only part of the Hamiltonian is maximized with respect to the thrust direction. The first reason is that it reduces the optimality condition from the root of a sixth- to third-order polynomial. The latter can be solved in closed form with consequent savings in machine time. The second reason is that it is unsatisfying aesthetically to bias the control so that the desired acceleration component is decreased while the thrust is increased. This result is mathematically time optimal because it increases the mass flow rate and reduces the mass. Although time-optimal solutions are of more practical interest than fuel optimal solutions, it does not seem desirable simply to throw fuel away.

This Appendix is intended to show that the suboptimal approximation is negligibly different from the time-optimal case for practical missions by analyzing the worst possible case. This case occurs when the radius vector to the spacecraft is always at right angles to the Earth-sun line and the primer vector is orthogonal to the Earth-sun line. A simple example of such a case is the coplanar enlargement of a circular orbit normal to the Earth-sun line. Such a case will be characterized by a 41% increase in ΔV and a 100% increase in flight time as compared to the unconstrained case. For the more practical examples treated in the body of this paper, the fuel and time penalties due to attitude constraints are much smaller than this. For these practical cases, the difference between the suboptimal and minimum time solutions will be smaller than for the extreme case treated herein.

This case may be characterized by only two state variables, the mean orbital speed v and the mass m. The rates of change of these two variables are

$$\dot{v} = -(2P_0/mc)\cos\psi\sin\psi \tag{A1}$$

$$\dot{m} = -(2P_0/c^2)\cos\psi \tag{A2}$$

The Hamiltonian of the problem is given by

$$H = -\lambda_v(2P_0/mc)\cos\psi\sin\psi - \lambda_m(2P_0/c^2)\cos\psi \tag{A3}$$

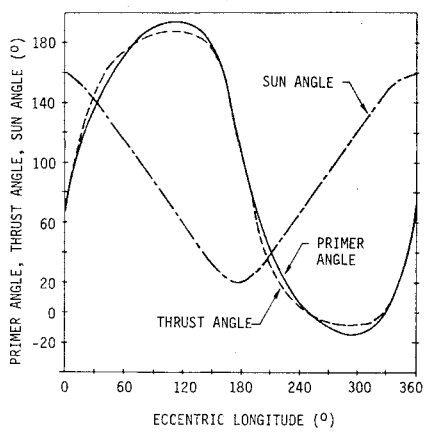

Fig. 7 Primer angle (α), thrust angle (ψ), and sun angle (β) for initial orbit.

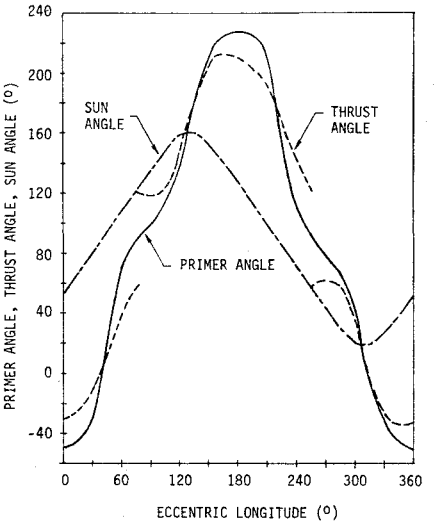

Fig. 8 Primer angle (α), thrust angle (ψ), and sun angle (β) for final orbit.

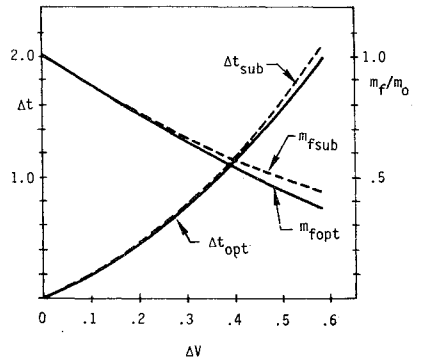

Fig. 9 Normalized time and mass change vs normalized velocity change.

The value of the yaw angle ψ that maximizes H is given by

$$\sin\psi^* = [\,(\lambda_m m/4\lambda_v c)^2 + \tfrac{1}{2}\,]^{\frac{1}{2}} - (\lambda_m m/4\lambda_v c) \qquad \text{(A4)}$$

The rates of change of the Lagrange multipliers are given by the canonical equations:

$$\dot{\lambda}_v = 0 \qquad \text{(A5)}$$

$$\dot{\lambda}_m = -\lambda_v\,(2P_0/m^2 c)\sin\psi\cos\psi \qquad \text{(A6)}$$

Three first integrals result from Eqs. (A5), (A7), and (A8). Equation (A7) follows from the autonomous nature of the problem, whereas Eq. (A8) follows from Eq. (A3):

$$\dot{H} = 0 \qquad \text{(A7)}$$

$$\mathrm{d}\lambda_m m/\mathrm{d}t = m\dot{\lambda}_m + \dot{m}\lambda_m = H \qquad \text{(A8)}$$

The three first integrals resulting from these equations are given by (A9-A11). The values of the integrals follow from the transversality conditions for a minimum time problem:

$$H = -1 \qquad \text{(A9)}$$

$$\lambda_m m = -(t - t_f) \qquad \text{(A10)}$$

$$\lambda_v = m_f c/P_0 \qquad \text{(A11)}$$

Substituting into Eq. (A4) yields. Eq. (A11):

$$\sin\psi^* = \left[\left[\frac{t-t_f}{4m_f c}P_0\right]^2 + \frac{1}{2}\right]^{\frac{1}{2}} + \frac{t-t_f}{4m_f c^2}P_0 \qquad \text{(A12)}$$

The problem now can be solved by quadrature to yield

$$m/m_f = 2\cos^2\psi\cot\psi \qquad \text{(A13)}$$

$$v_f - v = c(2)^{\frac{1}{2}} - 2\sin\psi + 3\ell n\{(\sec\psi + \tan\psi)/[1 + (2)^{\frac{1}{2}}]\} \qquad \text{(A14)}$$

$$t_f - t = (m_f c^2/2P_0)\,[4\sin\psi - 2\csc\psi] \qquad \text{(A15)}$$

The corresponding results for the suboptimal approximation used in the paper are given by

$$v_f - v = [c/(2)^{\frac{1}{2}}]\,\ell n(m/m_f) \qquad \text{(A16)}$$

$$t_f - t = [c^2/(2)^{\frac{1}{2}}P_0]\,(m - m_f) \qquad \text{(A17)}$$

The optimal and suboptimal cases are compared in Fig. 9, which plots the normalized time and mass against the normalized velocity change. The plot shows that the difference between the two cases is negligible for mass ratios characteristic of SERT-C (>0.84). For smaller mass ratios, the suboptimal approximation will take longer but use less fuel than the minimum-time case. For practical missions, the differences should be indistinguishable.

References

[1] Sackett, L.L. and Edelbaum, T.N., "Optimal High- and Low-Thrust Geocentric Transfer," AIAA Paper 74-801, Anaheim, Calif., Aug. 1974.

[2] Jasper, T.P., "Low-Thrust Trajectory Analysis for the Geosynchronous Mission," AIAA Paper 73-1072, Lake Tahoe, Calif., Oct. 1973.

[3] Williams, D.F., "MOLTOP Users Manual," M-240-1224, Oct. 1973, Northrup Services, Inc.

[4] Horsewood, J.L., Flanagan, P.F., and Mann, F.I., "Program Manual for the Systems Evaluation of Orbit Raising (SEOR)," 74-11, March 1974, Analytical Mechanics Associates, Inc., Seabrook, Md.

[5] "SERT C Project Study," NASA TMX-71508, Jan. 1974.

[6] Edelbaum, T.N., Sackett, L.L., and Malchow, H.L., "Optimal Low Thrust Geocentric Transfer," AIAA Paper 73-1074, Lake Tahoe, Calif., Oct. 1973.

[7] Sackett, L.L., and Malchow, H.L., and Edelbaum, T.N., "The Computation of Time Optimal Geocentric Transfers Using Solar or Nuclear Electric and High Thrust Propulsion," R-880, May 1975, The C.S. Draper Laboratory, Inc., Cambridge, Mass.

[8] Sackett, L.L., Edelbaum, T.N., and Malchow, H.L., "A Users Manual for a Computer Program which Calculates Time Optimal Geocentric Transfers Using Solar or Nuclear Electric and High Thrust Propulsion," R-827, June 1974, The C.S. Draper Laboratory, Inc., Cambridge, Mass.

[9] Sackett, L.L., Malchow, H.L., and Edelbaum, T.N., "Solar Electric Geocentric Transfer with Attitude Constraints: Analysis," R-901, Aug. 1975, The C.S. Draper Laboratory, Inc., Cambridge, Mass.

[10] Sackett, L.L., Malchow, H.L., and Edelbaum, T.N., "Solar Electric Geocentric Transfer with Attitude Constraints: Program Manual," R-902, Aug. 1975, The C.S. Draper Laboratory, Inc., Cambridge, Mass.

[11] Broucke, R.A. and Cefola, P.J., "On the Equinoctial Orbital Elements," *Celestial Mechanics*, Vol. 5, No.3, May 1972, pp. 303-310.

[12] Malchow, H.L. and Whitney, C.K., "A Radiation Model for Geocentric Trajectory Calculations," AIAA Paper 75-351, New Orleans, La., March 1975.